In vitro and *in silico* studies of prenylated phenylpropanoids of green propolis and their derivatives against cariogenic bacteria

Tatiana M. Vieira[a,†], Sara L. de Souza[b,†], Anna L. O. Santos[b,†], Ismail Daoud[c,d,†], Seyfeddine Rahali[e,†], Noureddine Amdouni[f,†], Julia G. Barco[a], Lucas A. L. Paula[g], Jairo K. Bastos[h], Carlos H. G. Martins[b], Ridha Ben Said[e,f],* Antônio E. M. Crotti[a,]*.

[a] *Department of Chemistry, Faculty of Philosophy, Science and Letters at Ribeirão Preto, University of São Paulo, 14040-901, Ribeirão Preto-SP, Brazil*

[b] *Department of Microbiology, Institute of Biomedical Sciences, Federal University of Uberlândia, Uberlândia-MG, Brazil*

[c] *University Mohamed Khider, Department of Matter Sciences, BP 145 RP, Biskra, Algeria*

[d] *Laboratory of Natural and Bio-active Substances, Faculty of Science, Tlemcen University, P.O. Box 119, Tlemcen, Algeria*

[e] *Department of Chemistry, College of Science and Arts at Ar Rass, Qassim University, P.O. Box 53, Ar Rass 51921, Saudi Arabia*

[f] *Laboratoire de Caractérisations, Applications et Modélisations des Matériaux, Faculté des Sciences de Tunis, Université Tunis El Manar, Tunis, Tunisia*

[g] *Center of Research on Natural Products, University of Franca, 14404-600, Franca-SP, Brazil*

[h] *School of Pharmaceutical Sciences of Ribeirão Preto, University of São Paulo, 14040-903, Ribeirão Preto-SP, Brazil*

[†] Authors who had the same contribution to this work

* Corresponding author: millercrotti@ffclrp.usp.br (A.E.M.C), ben.said.ridha@gmail.com (R.B.S)

Highlights

– Fourteen prenylated compounds and derivatives were synthesized, including artepillin C, drupanin, and plicatin B, which naturally occurs in Brazilian propolis;

– Plicatin B (**2**) and its hydrogenated **8** derivative displayed strong activity against *Streptococcus mutans*, *S. sanguinis*, and *S. mitis* (MIC = 31.2-62.5 µg/mL);

– Molecular docking studies revealed that complexes of compounds **2** and **8** with the active site residues of *S. mutans*, *S. mitis*, and *S. sanguinis* target have binding score energy values close to those of the native ligands due to the formation of strong hydrogen bonds;

– The calculated physicochemical parameters indicated that compounds **2** and **8** satisfy the criteria of drug-likeness without any violation of the Lipinski, Veber, and Egan rules;

– Compounds **2** and **8** exhibit suitable ADME-T parameters, as the online server pkCSM calculates.

Graphical Abstract

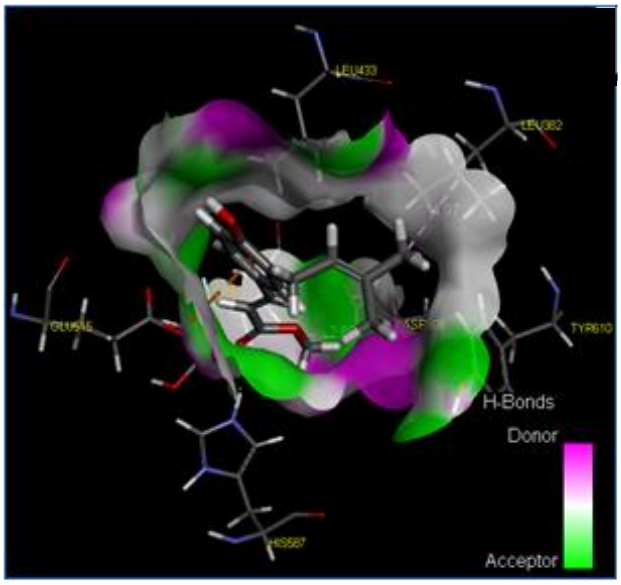

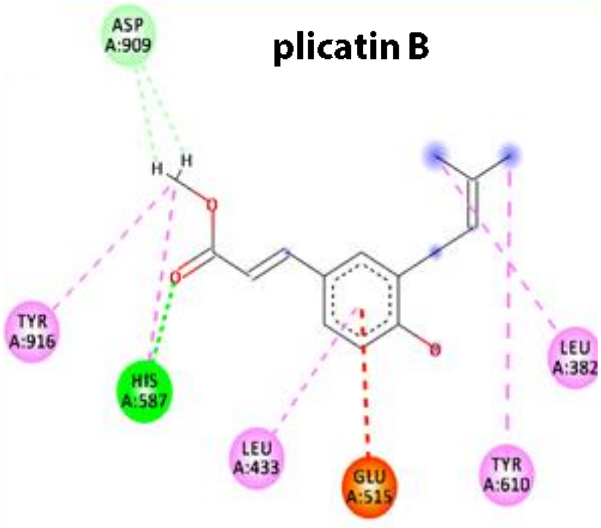

Abstract

Artepillin C, drupanin, and plicatin B are prenylated phenylpanoids naturally occurring in Brazilian green propolis. In this study, these compounds and eleven derivatives were synthesized and evaluated for their *in vitro* antimicrobial activity against a representative panel of cariogenic bacteria in terms of their minimum inhibitory concentration (MIC) values. Plicatin B (**2**) and its hydrogenated derivative **8** (2',3',7,8-tetrahydro-plicatin B) were the most active compounds. Plicatin B (**2**) displayed strong activity against all bacteria tested *(*MIC = 31.2 µg/mL). On the other hand, compound **8** (2',3',7,8-tetrahydro-plicatin A) displayed strong activity against *Streptococcus mutans, S. salivarius, S. sobrinus, Lactobacillus paracasei (*MIC = 62.5 µg/mL) and *S. mitis* (MIC = 31.2 µg/mL) as well as a moderate activity against *Enterococcus faecalis* and *S. sanguinis* (MIC = 125 µg/mL). *In silico* studies showed that the complexes formed compound **2** and **8** has energy score values close to those of the native ligands of *S. mitis*, *S. sanguinis*, and *S. mutans* due to the formation of strong hydrogen bonds with the active sites of those bacteria. Moreover, all the estimated physicochemical parameters satisfy the drug-likeness criteria without violating the Lipinski, Veber, and Egan rules, so these compounds are not expected to cause problems with oral bioavailability and pharmacokinetic parameters. Compounds **2** and **8** also have suitable ADME-T parameters, as the online server pkCSM calculates. These results make compounds **2** and **8** good candidates as anticariogenic compounds.

Keywords: artepillin C; cariogenic bacteria; molecular docking; oral pathogens; plicatin B; *Streptococcus mutans*

1. Introduction

Dental caries is an infectious disease that affects people worldwide, especially in low-income regions of developing countries [1]. The disease is characterized by a progressive and molecular disintegration of the dental structure, resulting from the accumulation of acidogenic and aciduric bacteria in the oral cavity to form the dental biofilm [2]. The most effective method of preventing dental biofilm is through mechanical removal by brushing and flossing [3]. However, in most cases, this mechanical method is performed improperly, especially in hard-to-reach places, such as sub-gums and fissures, which ends up favoring biofilm accumulation. Thus, the use of chemical methods, such as mouthwashes with antimicrobial action becomes necessary to promote the reduction of the adhesion of bacteria to the dental surface and inhibit cariogenic bacteria growth and proliferation [4,5]. Chlorhexidine is the most effective anti-cariogenic agent used in mouthwash formulationsto reduce plaque [5,6]. However, despite its effectiveness, chlorhexidine has shown adverse effects, especially in its daily use, in addition to the emergence of resistant strains [7,8]. In this scenario, the interest in new compounds with antimicrobial action as effective as chlorhexidine in controlling biofilm but with fewer adverse effects has grown in the last few years [9,10].

Propolis is a resinous product formed by plant material collected and deposited in hives by bees. The chemical composition of propolis depends on the botanical sources of each region [11]. Brazilian green propolis is produced by *Apis mellifera* using shoot apices of *Baccharis dracucunlifolia* (Asteraceae) in the country's Southeast [12]. Because of its wide diversity of biological and pharmacological activities [13-20], especially the antimicrobial properties [21-25], Brazilian green propolis has also been used in folk medicine and exported to several countries (e.g., Japan, China, Russia, France, and Germany) as sprays, toothpaste, soaps, ointments, and creams for skin [26].

Chemically, Brazilian green propolis is rich in prenylated compounds [27,28], mainly phenylpropanoids like drupanin (**I**), and artepillin C (**II,** Figure 1). These phenolic acids are commonly detected and identified in Brazilian green propolis [23,29-31]. In the literature, many studies have

reported the biological and pharmacological activities of artepillin C [23,29,32,33] and drupanin [30,31,34]. However, data on the antibacterial activity of these prenylated compounds against cariogenic bacteria are still scarce [35]

In this study, we investigated the antibacterial activity of a series of synthetic prenylated phenylpropanoids, including the naturally occurring compounds artepillin C and drupanin and their derivatives against a representative panel of cariogenic bacteria.

2. Material and Methods

2.1. Synthesis of artepillin C and derivatives

Compounds **1-4** were synthesized by alkylation of methyl *p*-coumarate according to the methodology employed by Patra and coworkers [36] with modifications (Scheme 1). In this procedure, methyl *p*-coumarate (0.5 mmol) was added to a 25-mL flask equipped with a magnetic stirrer bar. Next, 15 mL toluene was added. The mixture was cooled to 0°C, and 1.5 mmol NaH was added in portions. After 15 min, 1.5 mmol (153 µL) of prenyl bromide was added dropwise. The reaction progress was monitored through TLC using a Hex:EtOAc 8:2 (v/v) solution as the eluent. After 24 h, the solvent was removed under reduced pressure on a rotary evaporator, and the reaction mixture was then extracted with EtOAc (3 x 15 mL). The organic phase was washed with saturated NaCl solution (15 mL), dried over $MgSO_4$ and filtered off. The solvent was removed by evaporation at reduced pressure on a rota evaporator. The compounds were isolated by column chromatography with gradient elution starting with 100% hexane and changing to Hex:EtOAc 9.8:0.2 (v/v) after separation of the first compounds. The resulting solids were dried under vacuum to yield compounds **1** (32% yield), **2** (18% yield), **3** (15% yield), and **4** (35% yield) (Scheme 1).

Compounds **5**, **6**, and **7** were obtained from a hydrolysis reaction according to the methodology described by Uto and co-workers [37]. In this procedure, a solution of KOH (15 mL of a 10% aqueous) was added to a solution of the methyl esters **1, 2,** and **4** in MeOH (15 mL) (Scheme 1). The mixture

111 was heated under reflux for 1 h, cooled to 0-5 °C, and acidified with 1 mol/L HCl. After removing
112 MeOH under reduced pressure, the aqueous residue was extracted with EtOAc (3 x 15 mL). The
113 organic phase was washed with saturated NH_4Cl and brine, dried over $MgSO_4$, and evaporated under
114 reduced pressure. The resulting white solids were dried under vacuum, to afford compounds **5**, **6**, and
115 **7** in 100% yield.

116 Compounds **8**, **9, 12**, **13**, and **14** were obtained from **3**, **4**, **5, 6,** and **7** by catalytic hydrogenation.
117 In this procedure, compounds **2**, **3**, **5**, **6**, and **7** and Pd/C (catalyst) were wholly dissolved in HPLC
118 grade EtOAc and transferred to a high-pressure reactor under stirring and kept under H_2 atmosphere,
119 and 400 psi at room temperature for 1-2 h (Scheme 1). The resulting oil was dried under vacuum, to
120 yield compounds **8**, **9, 12**, **13**, and **14** in 100% yield.

121 Compounds **10** and **11** were synthesized according to the methodology by Kantee and co-
122 workers [38] with some modifications (Scheme 1). In this procedure, $LiAlH_4$ (0.68 mmol) was quickly
123 added to a solution of compounds **3** and **4** (0.34 mmol) in THF (5.5 mL) at 0 °C. The reaction mixture
124 was stirred under an N_2 atmosphere at 0 °C for 1 h. After one hour, the mixture was allowed to stir at
125 room temperature for 9-10 h. The reaction mixture was then added H_2O, conc. HCl and extracted with
126 EtOAc (x3). The combined organic layers were washed with brine, dried over $MgSO_4$, and
127 concentrated under vacuum. Purification of the crude residue by column chromatography with
128 isocratic elution with Hex/EtOAc 9.8:0.2 (v/v) gave the corresponding alcohol derivative. The
129 resulting compounds were dried under vacuum, to yield compounds **10** (65% yield) and **11** (89%
130 yield).

131

132 *2.2. Antibacterial Assays*

133 The *in vitro* antimicrobial action of artepillin C (**5**), drupanin (**6**) and derivatives **1-4**, and **7-14**
134 was evaluated in terms of their minimum inhibitory concentration (MIC) values [39], which were
135 interpreted as the lowest concentrations that inhibited bacterial growth. To this end, *Streptococcus*

mutans (ATCC 25175), *Streptococcus mitis* (ATCC 49456), *Streptococcus salivarius* (ATCC 25975), *Streptococcus sanguinis* (ATCC 10556), *Streptococcus sobrinus* (ATCC 33478), *Enterococcus faecalis* (ATCC 4082), and *Lactobacillus paracasei* (ATCC 11578) were assayed by the broth microdilution method, in 96-well microplates. The bacterial colonies were cultured at 37 ºC for 24 h in blood agar (Difco Labs, Detroit, MI, USA). Further standardization of the inoculum quantity was accomplished on a spectrophotometer Femto (São Paulo, Brazil) operating at a wavelength of 625 nm, to match 0.5 in the McFarland scale (1.5 x 10^8 CFU/mL). The microorganism suspensions were diluted to a final concentration of 5 x 10^5 CFU/mL. Samples of compounds **1-14** were dissolved in DMSO (Merck, Darmstadt, Germany) and tryptic soy broth (TSB, Difco) to obtain final concentrations varying from 0.98 to 2000 µg/mL. Inoculated microplate wells containing DMSO (1%) and TSB (1:5 v/v and 100%) were employed as the negative control. A non-inoculated well was also added to ensure medium sterility. Chlorhexidine (Sigma-Aldrich, St. Louis) was used as the positive control at concentrations ranging from 0.115 to 59 µg/mL in TSB (Difco). The microplates were sealed with plastic film and incubated at 37 ºC for 24 h. Next, 30 µL of revealing 0.02% resazurin (Sigma-Aldrich, St. Louis) was added to each microplate well, to indicate microbial viability. Before resazurin was added and to determine the MBC, a 10-µL aliquot of the inoculum was aseptically removed from each well and plated onto blood agar (Difco). The plates were incubated as described previously. The Minimum Bactericidal Concentration (MBC) was determined as the lowest compound concentration that killed > 99.9% of the initial bacteria population, at which no visible bacterial growth occurred [40]. MIC values were assessed by analysis of the color change of the resazurin solution from blue (without metabolic activity) to pink (with metabolic activity) [41]. The MIC and MBC were determined in triplicate for each microorganisme, and the results were presented as a mean ± standard deviation

2.3. Computational Methodology

2.3.1. Ligands and targets preparation

The 3D structures of the most active compounds **2** and **8** (Scheme 1) were optimized using the semi-empirical method AM1 [42], which was implemented in Hyperchem 8.0.8 software (Version 8.0.8, Hypercube, USA, http://www.hyper.com). Next, the 3D structures were converted into format.*mdb to use as input MOE-docking.

The crystal structures of *S. mitis* (PDB ID: **3LE0**) [43], *S. sanguinis* (PDB ID: **4N82**) [44], and *S. mutans* (PDB ID: **3AIC**) [45] were selected as antibacterial targets, which were downloaded from Protein Data Bank (http://www.rcsb.org/pdb/). Some information related to the target structures is given in Table 1.

2.3.2. Docking method protocol and validation

The molecular docking studies were carried out to identify the binding interactions of the most active compounds **2** and **8** within the binding site residue of the targets by using MOE software [46], and the docking protocol steps were followed and detailed in our previous research [47,48] by using the following default parameters; Placement: Triangle Matcher; Rescoring 1: London dG scoring function.

The re-dock of all native ligands to their targets was conducted using "Dock Option" implemented in the MOE software [46] to validate the used method. The RSMD values of the obtained complexes (Targets-Crystallized ligands) were less than 2.50 Å [49], meaning that the docking method is accurate and successful.

2.3.3. Molecular Dynamics (MD) and Simulation

MD simulations were carried out using the "Compute/Simulations/Dynamics" options in the MOE 2014.0901 software [46] to study the stability of the two best-formed complexes. The following default parameters were used: The Nose–Poincaré–Andersen (NPA) algorithm to search the interactions of different residues in each system, and MMFF94x force field used for the energy

minimization step of these complexes [50,51]. The MD protocol was settled for 1500 ps (an equilibrium period of 100 ps followed by a production period of 1400 ps, at a constant temperature of 310 K). Finally, the plots of potential energies U (kcal/mol) variations as a function of time t (ps) were taken by using OriginPro 9.1.software [52].

2.3.4. ADME-Tox evaluation

The drug-likeness rules, namely Lipinski, Veber, and Ghose, were verified by calculating the different physicochemical parameters (Total Polar Surface Area (TPSA); Number of Rotatable Bonds (nROTB), Molecular Weight (MW), lipophilicity (LogP), Number of hydrogen bond acceptors (nHA), and Number of hydrogen bond donors (nHD)) using the SwissADME server (http://www.swissadme.ch/) [53].

The pkCSM server (http://biosig.unimelb.edu.au/pkcsm/prediction) [54] was used for the analysis of ADMET profiles by calculating the following parameters: The **Absorption** (Caco-2: Colon adenocarcinoma**,** HIA: Human Intestinal Absorption**)**, **Distribution** (CNS: Central Nervous System permeability, BBB: Blood–Brain Barrier permeability), **Metabolism** (CYP1A2 inhibitor, CYP2C19 inhibitor, CYP2D6 inhibitor), **Excretion** (Renal OCT2 substrate: Organic cation transporter 2, Total Clearance) and **Toxicity** (hERG: Human Ether-a-go-go-Related Gene, Hepatotoxicity).

3. Results and Discussion

3.1. In vitro *antibacterial activity of compounds* ***1-14***

Artepillin C (**5**), drupanin (**6**), and compounds **7-14** were obtained by hydrolysis, reduction with $LiAlH_4$, and/or catalytic hydrogenation of prenylation products of methyl *p*-coumarate **1-4**, as shown in Scheme 1. Table 2 summarizes the results of the antimicrobial assays with the fourteen compounds against a representative panel of cariogenic bacteria regarding their minimum inhibitory concentration (MIC) and minimum bactericidal concentration (MBC). The antimicrobial activity was classified

based on the MIC values, as follows: MIC values lower than 10 µg/mL, between 11 and 100 µg/mL, between 101 and 500 µg/mL, and between 501 and 1000 µg/mL correspond to very strong, strong, moderate, and weak activities respectively, while MIC values higher than 1000 µg/mL denote inactivity [55-58]. Based on these criteria, compounds **2** and **8** displayed strong or moderate activity against all tested bacteria (Table 2). However, the lowest MIC value was observed **2** (plicatin B), which showed strong activity against *Streptococcus mutans*, *S. mitis*, and *S. sanguinis* (MIC = 31.2 µg/mL). This compound also showed strong activity against *S. salivarus* and *S. sobrinus* (MIC = 62.5 µg/mL). The strong activity of compound **2** against *S. mutans* is an auspicious result because it is one of the leading agents causing dental caries [55]. Artepillin C (**5**) and drupanin (**6**), which are among the most common prenylated compounds in Brazilian green propolis, showed moderate or weak activity against most of the tested bacteria (MIC between 125 and 1000 µg/mL), with drupanin displaying MIC values slightly lower than artepillin C. Plicatin B (**2**), has been isolated from Brazilian propolis samples, even though its occurrence is less commonly reported [59]. However, data on the antimicrobial activity of plicatin B are still scarce in the literature [60]. On the other hand, compounds **1**, **10**, and **14** had no activity against any of the cariogenic bacteria tested, with MIC values higher than 1000 µg/mL (data not shown in Table 2).

Aga and coworkers compared the antimicrobial activity of artepillin C with that of 3-prenyl-4-hydroxycinnamic acid and 4-hydroxycinnamic acid. They considered that the antimicrobial activity of this class of compounds may be increased by an increasing number of prenyl groups in the structure [25]. Herein, the results obtained showed that the mono-prenylated ester **2** (plicatin B), and its homolog carboxylic acid **6** (drupanin) are more active against the tested cariogenic bacteria than the di-prenylated compounds **1** and **5** (artepillin C), respectively. It indicated clearly that other structure features than the prenyl groups also play a key role in the antibacterial activity of compounds **1-14**. Indeed, the comparison between the MIC values of the isomers **2** (a C-prenylated compound) and **4** (an *O*-prenylated compound) revealed that the phenolic hydroxyl is a crucial structure feature for the

antibacterial activity, likely due to its capability to make a hydrogen bond to the active binding sites of the bacteria enzymes, thus inhibiting microbial enzymes and simultaneously increasing affinity to cytoplasmic membranes [61]. This is reinforced by the fact that compound **3** (a tri-prenylated ester that contains a prenyl group at the oxygen at C4) is less active against the selected cariogenic bacteria as compared to **2** (a mono-*C*-prenylated ester), despite its higher lipophilicity. On the other hand, the effect of the nature of the oxygenated function at C9 and the type of covalent bond between C7 and C8 cannot be analyzed individually. For example, the methyl esters **2** (plicatin B) and its hydrogenated derivative **8** are more active than their corresponding carboxylic acids **7** (drupanin) and **13**, indicating that the presence of an ester function at C9 potentializes the antibacterial activity of mono-*C*-prenylated compounds. In contrast, in the case of compounds di-*C*-prenylated **5** (artepillin C) and *O*-prenylated **7**, the carboxyl group at C9 increases the antibacterial activity as compared to the corresponding methyl esters **1** and **4**. Similarly, the presence of a single bond between C7 and C8 in the structure of mono-*C*-prenylated compounds **8** (a methyl ester) and **13** (a carboxylic acid) decreases the antibacterial activity as compared to compounds **2** and **6**, which display a double bond between C7 and C8. On the other hand, for compounds di- and tri-prenylated **12** and **9**, a single bond between C7 and C8 increases the antibacterial activity as compared to **5** and **3**, respectively.

According to literature, the mechanism by which phenolic acids enter the molecular structure of the bacteria membrane involves the orientation of the phenol hydroxyl into the aqueous phase by hydrogen bonding, and the non-polar carbon chain alignment into the lipid phase by dispersion forces. The activity tends to disappear when the hydrophilic force exceeds the hydrophobic one [62]. Therefore, the antibacterial activity of compounds **1-14** depends on the balance between hydrophilicity/lipophilicity. In this sense, it can be inferred that compounds **2** and **8** achieve the best lipophilicity/hydrophilicity balance among the tested compounds. Hydrolysis of plicatin B (**2**) produces drupanin (**6**), which has a carboxyl group at C9. Although this group can anchor the compound to the lipid bilayer [63], it also increases the hydrophilicity of drupanin (**6**) as compared to

plicatin B (**2**) and consequently decreases its antibacterial activity. On the other hand, the *C*-prenyl groups in the structure of artepillin C (**5**) drastically increase lipophilicity as compared to **2** and **6**, thus decreasing its antibacterial activity. Finally, the presence of an α,β-unsaturated carbonyl conjugated with the aromatic ring of phenylpropanoids **1-7** confers conformational and electronic characteristics that are strongly influenced by the phenol-OH group in *para* position [64]. In principle, because of the rotation around the single bond between C7 and C8, compounds **8**, **9**, **12**, **13**, and **14** can assume a wider variety of conformations as compared to **1-7**, **10**, and **11**, and improve their intermolecular interactions with a potential target [65]. However, data from this study suggested a combined effect of the nature of the bond between C7 and C8 and the number and position of the prenyl groups on the molecular shape and, consequently, the antibacterial activity of compounds **1-14**.

*3.2. In silico studies on the antibacterial activity of **2** and **8***

3.2.1. Target-compounds interactions

The docking simulation results for compounds **2** and **8**, along with both X-ray crystals of the studied targets are listed in Table 3. The visualization of all possible interactions that have been formed between compounds and receptor active site residues was generated by the BIOVIA DS visualize package (Dassault Systèmes BIOVIA, Discovery Studio Modeling Environment, 2020).

Based on the binding score energy values, compounds **2** and **8** were more potent inhibitors of *S. mitis* (PDB ID: 3LE0) than the native ligand (GOL). The complexes formed by these compounds have low score energy values of -4.228, and -4.476 kcal/mol, respectively (Table 3). However, compound **8** was predicted to be the strongest *S. mitis* (PDB ID: 3LE0) target binder as compared to compound **2,** which forms the complex with high stability, confirmed by the negative score energy of -4.476 kcal/mol. These results suggest that compound **8** has a high affinity with the pocket of *S. mitis* (PDB ID: 3LE0), which is confirmed by establishing four strong hydrogen bonds [66,67] with active site residue of *S. mitis* (PDB ID: 3LE0) target: one Conventional H-bond type (H/ HIS85(A)-NE2/

bond distance= 2.23Å), and three other carbon H-bonds (H/ ASP114(A)-OD1/bond distance = 2.87Å, H/ ASP77(A)-OD2/bond distance = 2.90Å), and H/ ASP114(A)-OD1/bond distance = 2.95Å). One electrostatic interaction with ARG112(A) was also observed. On the other hand, this compound formed one hydrophobic interaction with the enzyme's active site (Table 3+Figure 2B). Recent studies have revealed that residues ARG112(A) and HIS85(A) play an essential role in the inhibition of S. *mitis* (PDB ID: 3LE0) target [68,69].

It is noteworthy that in the case of *S. sanguinis* (PDB ID: 4N82) target, the complex formed by compound **2** gave a high negative score energy value (-6.156 kcal/mol) as compared to compound **8** (Table 3). In addition, the score value of compound **2** (-6.156 kcal/mol) is very close to the native ligand FMN (-6.671 kcal/mol) (Table 3). The docked conformation of compound **2** with *S. sanguinis* (PDB ID: 4N82) target is shown in Figure 3A. It can be noted that this compound makes two strong carbon H-bonds (O/ASN104(A)-H/bond distance = 2.37Å, and O/GLY103(A)-HA3/bond distance = 2.93Å), besides one Pi-Lone Pair interaction (with TYR63(A)) and four hydrophobic interactions with residues PHE107(A), MET132(A), PRO62(A), and TYR64(A) (Table 3+Figure 3A). Furthermore, some papers reported that all these residues affect the formed complex stability [44,68].

In the case of *S. mutans* (PDB ID: **3AIC**), it can be observed that the complexes formed by compounds **2** and **8** have low score energy values of -5.049 and -5.042 kcal/mol, respectively, which are similar to those of the native ligand, acarbose (-6.674 kcal/mol, Table 3). Furthermore, compound **2** fits nicely into *S. mutans* (PDB ID: **3AIC**) pocket due to three strong hydrogen bonds [66,67] with active site residue of *S. mutans* (PDB ID: **3AIC**) target: one conventional H-bond type (O/HIS587(A)-HE2/ bond distance= 2.04 Å) and two other carbon H-bonds (H/ASP909(A)-OD1/bond distance = 2.85Å, and H/ASP909(A)-OD1/bond distance = 2.74 Å). An electrostatic interaction with GLU515(A) was also observed. In contrast, this compound formed five hydrophobic interactions with the following active site residues: LEU382(A), HIS587(A), TYR610(A), TYR916(A), and LEU433(A) (Table 3+Figure 4A). This result was supported by several recent studies [70-72].

311

312 3.2.2. Molecular Dynamics Simulation

313 The MD simulations were performed to investigate the stability of the best complexes
314 obtained through molecular docking calculations, such as (**a**):3LE0-L5, (**b**):4N82-L4, and (**c**) 3AIC-
315 L4. Figure 4 presents the 3D diagrams of the best pose for compounds **2** and **8** with the active binding
316 sites 3LE0, 4N82, and 3AIC, as determined by molecular docking (green) and molecular dynamics
317 (yellow) studies

318 According to Figure 5, a fluctuation in all curves was initially observed during the first 100
319 picoseconds, which can be justified by the variation of the potential energy of three complexes: 3LE0-
320 Compound **2**, (**d**): 4N82-Compound **2**, and 3AIC- Compound **2**. A slight variation in potential energy
321 was observed between 100 and 800 ps in curve (a), and between 100 and 400 ps in curve (e), and
322 between 100 and 900 ps in curve (c). Finally, the 3LE0-Compound **8,** 4N82-Compound **8**, and 3AIC-
323 Compound **8** complexes retain their stabilities in the last intervals (between 800 and 1500 ps, between
324 400 and 1500 ps, and between 900-1500 ps, respectively) (Figure 5a, b, and c). On the other hand, all
325 the studied complexes exhibit higher stability, confirmed by MD simulations, because they maintained
326 almost the same types of interactions compared to the molecular docking studies, which was also
327 confirmed by the stability of the potential energy as a function of time (Figure 5a, b, and c), as reported
328 in recent papers [73,74].

329

330 3.2.3. ADMET and drug-likeness prediction

331 3.2.2.1. Drug-likeness evaluation

332 Different parameters of physicochemical properties were calculated for compounds **2** and **8,**
333 aiming to verify the drug-likeness rules using the SwissADME online server (Table 4).

334 As shown in Table 4, it is apparent that compounds **2** and **8** have several hydrogen bond donors
335 <5 **(**n-HD: 0~7**)** and hydrogen bond acceptors <10 **(**n-HA: 0~10**)**. In addition, the Molecular Weight

values of these compounds belong to the interval 100~500 g/mol, and their MLogP and WLogP values are <5. Also, the nROTB values are <11, which denotes the flexibility of these compounds. Moreover, the TPSA values obtained for both compounds are less than 140 Å. Therefore, compounds **2** and **8** satisfy the drug-likeness criteria without violating the Lipinski, Veber, and Egan rules. Furthermore, based on these results, these compounds are not expected to cause problems with oral bioavailability and pharmacokinetic parameters.

3.2.2.2. ADME-T properties

The Absorption, Distribution, Metabolism, Excretion, and Toxicity (ADME-T) were calculated for compounds **2** and **8** using the online server pkCSM (Table 5). The Caco-2 values obtained for **2** and **8** are higher than -5.15 (>-5.15 cm/s), which confirmed that these compounds have good permeability. Moreover, both compounds have HIA values higher than 30%, which means that compounds **2** and **8** administered orally can be absorbed from the gastrointestinal system into the human body's bloodstream. The logPS values (-3< logPS <-2) indicate that compounds **2** and **8** cannot penetrate the CNS. Additionally, the logBB values of compounds **2** (0.311), and **8** (0.030) indicate that compound **2** is expected to readily cross the blood-brain barrier, whereas compound **8** is poorly distributed in the brain (Table 5). Compounds **2** and **8** are CYP1A2 inhibitors, and not CYP2C19 and CYP2D6 inhibitors. In addition, these compounds are not CYP2D6 and CYP3A4 substrates and are not likely an OCT2 substrate. These compounds are also expected to have a low clearance (<5 mL/min /kg) (Table 5). Furthermore, compounds **2** and **8** are neither hERG I nor hERG II inhibitors, showing no hepatotoxicity risk.

4. Conclusions

Plicatin B was identified as a compound with promising activity against cariogenic bacteria, including *Streptococcus mutans*, one of the main bacteria caries causatives. Moreover, this study revealed that plicatin B was shown to be more active than artepillin C, which has been highlighted as the main responsible for the antimicrobial activity of the Brazilian green propolis. However, among all the tested compounds, the most remarkable activity against *S. mutans* was the hydrogenation product of plicatin B. Studies to explore the structure-activity relationships of artepillin C and its derivatives more deeply are underway.

The present research has revealed that the most active compounds **2** and **8** can be considered lead candidates for inhibiting the two targets. The investigation was carried out by molecular docking/dynamics analyses and ADME prediction, which were successfully used to discover a new class of antibacterial inhibitors. The molecular docking/dynamics simulation results proved that compounds 4 and 5 have high binding affinities against three targets *S. sanguinis* (PDB ID: 4N82) and *S. mitis* (PDB ID: 3LE0), confirmed by low score energy values and various interactions with the active site residues of these targets.

ADME-T properties were predicted for all candidates to validate the pharmacodynamics and pharmacokinetics profiles, and these compounds verified the three rules, Lipinski, Veber, and Egan.

Acknowledgments

The authors thank the São Paulo Research Foundation (FAPESP, grants 19/11700-0 and 17/04138-8) for the financial support and scholarships, and to National Council for Scientific and Technological Development (CNPq, proc. 301417/2019-9) for fellowships.

References

[1] A. Teshome, A. Muche, B. Girma, Prevalence of dental caries and associated factors in East Africa, 2000–2020: Systematic review and meta-analysis, Front. Publ. Health 9 (2021) 645091, https://doi.org/10.3389/fpubh.2021.645091.

[2] L. Tahir, R. Nazir, Dental caries, etiology, and remedy through natural resources, in: Z. Akarslan (Ed.), Dental caries, IntechOpen, London, UK, 2019, pp. 19-33.

[3] S.R. Sahoo, D.B. Nandini, P.S. Basandi, M. Selvamani, M. Donoghue, A Comparison of pre- and postbreakfast tooth brushing in caries prevention through the estimation of *Streptococcus mutans* counts: a prospective clinical and microbiological study, J. Microsc. Ultrastruct. 10(4) (2022) 168-173, https://doi.org/10.4103/jmau.jmau_90_21.

[4] D. Kamal, H. Hassanein, M. Akah, M.A. Abdelkawy, H. Hamza, Caries preventive and antibacterial effects of two natural mouthwashes vs chlorhexidine in high caries-risk patients: a randomized clinical trial, J. Contemp. Dent. Pract. 21(12) (2020) 1316-1324, https://doi.org/10.5005/jp-journals-10024-2986.

[5] E. Fibryanto, L. Santoso, Mouthwashes: a review on its efficacy in preventing dental caries, JKGT 5(1) (2023) 91-96, https://doi.org/10.25105/jkgt.v5i1.16891.

[6] A. Masapu, S.S.M. Kumar, K.P. Ashok, G. Anusha, J. Sangineedy, S. Ashok, Evaluation of the antiplaque efficacy of chlorhexidine mouthwash immediately and 30 min after brushing with fluoride toothpaste - a pilot study, RGUHS J. Dent. Sci. 11(2) (2019) 17-21, https://doi.org/10.26715/rjds.11_2_4.

[7] S. Busxer, Has resistance to chlorhexidine increased among clinically-relevant bacteria? A systematic review of time course and subpopulation data, PLoS One 16(8) (2021) e0256336, https://doi.org/10.1371/journal.pone.0256336.

[8] F. Cieplik, N.S. Jakubovics, W. Buchalla, T. Maisch, E. Hellwig, A. Al-Ahmad, Resistance toward chlorhexidine in oral bacteria – is there cause for concern?, Front. Microbiol. 10(587) (2019) 587, https://doi.org/10.3389/fmicb.2019.00587.

[9] A. Fahim, W.H. Himratul-Aznita, P.S. Abdul-Rahman, Allium-sativum and bakuchiol combination: A natural alternative to Chlorhexidine for oral infections?, Pakistan J. Med. Sci. 36(2) (2020) 271-275, https://doi.org/10.12669/pjms.36.2.1457.

[10] K.H. Soares, P. Firoozi, G.M. Souza, B.L. Martins, S.G.M. Falci, C.R.R. Santos, Efficacy of probiotics compared to chlorhexidine mouthwash in improving periodontal status: a systematic review and meta-analysis, Int. J. Dent. 2023 (2023) Article ID 4013004, https://doi.org/10.1155/2023/4013004.

[11] R. Hossain, C. Quispe, R.A. Khan, A.S.M. Saikat, P. Ray, D. Ongalbek, B. Yeskaliyeva, D. Jain, A. Smeriglio, D. Trombetta, R. Kiani, F. Kobarfard, N. Mojgani, P. Salfarian, S.A. Ayatollahi, C. Sarkar, M.T. Islam, D. Keriman, A. Uçar, M. Martorell, A. Sureda, G. Pintus, M. Butnariu, J. Sharifi-Rad, W.C. Cho, Propolis: An update on its chemistry and pharmacological applications, Chin. Med. 17(100) (2022) 651, https://doi.org/10.1186/s13020-022-00651-2.

[12] E.W. Teixeira, G. Negri, R.M.S.A. Meira, D. Message, A. Salatino, Plant origin of green propolis: Bee behavior, plant anatomy and chemistry, Evid. Based Compl. Altern. Med. 2(1) (2005) 85-92, https://doi.org/10.1093/ecam/neh055.

[13] P. Costa, L.B. Somensi, R. da Silva, L.N.B. Mariano, T. Boeing, B. Longo, E. Perfoll, P. de Souza, L.F.S. Gushiken, C.H. Pellizzon, D.M. Rodrigues, J.K. Bastos, S.F. de Andrade, L.M. Silva, Role of the antioxidant properties in the gastroprotective and gastric healing activity promoted by Brazilian green propolis and the healing efficacy of Artepillin C, Inflammopharmacology 28(4) (2020) 1009-1025, https://doi.org/10.1007/s10787-019-00649-7.

[14] P.F. de Oliveira, I.M.D. Lima, C.C. Munari, J.K. Bastos, A.A. da Silva, D.C. Tavares, Comparative evaluation of antiproliferative effects of Brazilian green propolis, its main source *Baccharis dracunculifolia*, and their major constituents artepillin c and baccharin, Planta Med. 80(6) (2014) 490-492, https://doi.org/10.1055/s-0034-1368298.

[15] J.L. Ding, T. Matsumiya, R. Hayakari, Y. Shiba, S. Kawaguchi, K. Seya, K. Ueno, T. Imaizumi, Daily Brazilian green propolis intake elevates blood artepillin C levels in humans, J. Sci. Food Agric. 101(11) (2021) 4855-4861, https://doi.org/10.1002/jsfa.11132.

[16] T. Kimoto, S. Koya-Miyata, K. Hino, M.J. Micallef, T. Hanaya, S. Arai, M. Ikeda, M. Kurimoto, Pulmonary carcinogenesis induced by ferric nitrilotriacetate in mice and protection from it by Brazilian propolis and artepillin C, Virchows Archiv. Int. J. Phatol. 438(3) (2001) 259-270, https://doi.org/10.1007/s004280000350.

[17] M. Klosek, L. Sedek, H. Lewandowska, Z.P. Czuba, The effect of ethanolic extract of Brazilian green propolis and artepillin C on aFGF-1, Eselectin, and CD40L secreted by human gingival fibroblasts, Cent. Eur. J. Immunol. 46(4) (2021) 438-445, https://doi.org/10.5114/ceji.2021.111215.

[18] K. Naramoto, M. Kato, K. Ichihara, Effects of an ethanol extract of Brazilian green propolis on human cytochrome P450 enzyme activities *in vitro*, J. Agr. Food Chem. 62(46) (2014) 11296-11302, https://doi.org/10.1021/jf504034u.

[19] N. Paulino, S.R.L. Abreu, Y. Uto, D. Koyama, H. Nagasawa, H. Hori, V.M. Dirsch, A.M. Vollmar, A. Scremin, W.A. Bretz, Anti-inflammatory effects of a bioavailable compound, Artepillin C, in Brazilian propolis, Eur. J. Pharmacol. 587(1-3) (2008) 296-301, https://doi.org/10.1016/j.ejphar.2008.02.067.

[20] M.R. Ahn, K. Kunimasa, T. Ohta, S. Kumazawa, M. Kamihira, K. Kaji, Y. Uto, H. Hori, H. Nagasawa, T. Nakayama, Suppression of tumor-induced angiogenesis by Brazilian propolis: Major component artepillin C inhibits *in vitro* tube formation and endothelial cell proliferation, Cancer Lett. 252(2) (2007) 235-243, https://doi.org/10.1016/j.canlet.2006.12.039.

[21] J.B. Seibert, J.P. Bautista-Silva, T.R. Amparo, A. Petit, P. Pervier, J.C.D. Almeida, M.C. Azevedo, B.M. Silveira, G.C. Brandao, G.H.B. de Souza, L.F.D. Teixeira, O.D.H. dos Santos, Development of propolis nanoemulsion with antioxidant and antimicrobial activity for use as

a potential natural preservative, Food Chem. 287 (2019) 61-67, https://doi.org/10.1016/j.foodchem.2019.02.078.

[22] R.M. Souza, M.C. de Souza, M.L. Patitucci, J.F.M. Silva, Evaluation of antioxidant and antimicrobial activities and characterization of bioactive components of two Brazilian propolis samples using a pK(a)-guided fractionation, Z. Naturforsch. C 62(11-12) (2007) 801-807,

[23] R.S. Veiga, S.D. Mendonça, P.B. Mendes, N. Paulino, M.J. Mimica, A.A. Lagareiro Netto, I.S. Lira, B.G.C. López, V. Negrão, M.C. Marcucci, Artepillin C and phenolic compounds responsible for antimicrobial and antioxidant activity of green propolis and *Baccharis dracunculifolia* DC, J. Appl. Microbiol. 122 (2017) 911-920, https://doi.org/10.1111/jam.13400.

[24] R. Jorge, N.A.J.C. Furtado, J.P.B. Sousa, A.A. da Silva, L.E. Gregorio, C.H.G. Martins, A.E.E. Soares, J.K. Bastos, W.R. Cunha, M.L.A. Silva, Brazilian Propolis: seasonal variation of the prenylated p-coumaric acids and antimicrobial activity, Pharm. Biol. 46(12) (2008) 889-893, https://doi.org/10.1080/13880200802370373.

[25] H. Aga, T. Shibuya, T. Sugimoto, M. Kurimoto, S. Nakajima, Isolation and identification of antimicrobial compounds in Brazilian propolis, Biosci. Biotech. Biochem. 58 (1994) 945-946, https://doi.org/10.1271/bbb.58.945.

[26] A.C.H.F. Sawaya, I.B.S. Cunha, M.C. Marcucci, Analytical methods applied to diverse types of Brazilian propolis, Chem. Cent. J. 5 (2011) 27, https://doi.org/10.1186/1752-153X-5-27.

[27] A.A. Righi, G. Negri, A. Salatino, Comparative chemistry of propolis from eight Brazilian localities, Evid. Based Compl. Altern. Med. 2013 (2013) 267878, https://doi.org/0.1155/2013/267878.

[28] A. Salatino, E.W. Teixeira, G. Negri, D. Message, Origin and chemical variation of Brazilian propolis, Evid. Based Compl. Altern. Med. 2(1) (2005) 33-38, https://doi.org/10.1093/ecam/neh060.

[29] M. Shahinozzama, B. Basak, R. Emran, P. Rozario, D.N. Obanda, Artepillin C: a comprehensive review of its chemistry, bioavailability, and pharmacological properties, Fitoterapia 147 (2020) 104775, https://doi.org/10.1016/j.fitote.2020.104775.

[30] P. Costa, M.O. Almeida, M. Lemos, C. Arruda, R. Casoti, L.B. Somensi, T. Boeing, M. Mariott, R. da Silva, B.D. Stein, P. de Souza, A.C. dos Santos, J.K. Bastos, L.M. da Silva, S.F. de Andrade, Artepillin C, drupanin, aromadendrin-4'-O-methyl-ether and kaempferide from Brazilian green propolis promote gastroprotective action by diversified mode of action, J. Ethnopharmacol. 226 (2018) 82-89, https://doi.org/10.1016/j.jep.2018.08.006.

[31] S. Mishima, Y. Ono, Y. Araki, Y. Akao, Y. Nozawa, Two related cinnamic acid derivatives from Brazilian honey bee propolis, baccharin and drupanin, induce growth inhibition in allografted sarcoma S-180 in mice, Biol. Pharm. Bull. 28(6) (2005) 1025-1030, https://doi.org/10.1248/bpb.28.1025.

[32] G.O. Estrada, J.F. da Silva, O.A. Antunes, Artepillin C: A review, Letters in Drug Design & Discovery 5(2) (2008) 88-92,

[33] Y. Kano, N. Horie, S. Doi, F. Aramaki, H. Maeda, F. Hiragami, K. Kawamura, H. Motoda, Y. Koike, J. Akiyama, S. Eguchi, K. Hashimoto, Artepillin C derived from propolis induces neurite outgrowth in PC12m3 cells via ERK and p38 MAPK pathways, Neurochem. Res. 33(9) (2008) 1795-1803, https://doi.org/10.1007/s11064-008-9633-9.

[34] D.M. Rodrigues, G.B. Portapilla, G.M. Silva, A. Duarte, C.G. Rotta, C. Silva, S. de Albuquerque, J.K. Bastos, V.L. Campo, Synthesis, antitumor activity and *in silico* analyses of amino acid derivatives of artepillin C, drupanin and baccharin from green propolis, Bioorg. Med. Chem. 47 (2021) 116372, https://doi.org/10.1016/j.bmc.2021.116372.

[35] A.P. Tiveron, P.L. Rosalen, M. Franchin, R.C.C. Lacerda, B. Bueno-Silva, B. Benso, C. Denny, M. Ikegaki, S.M. Alencar, Chemical characterization and antioxidant, antimicrobial, and anti-

inflammatory activities of South Brazilian organic propolis, PLoS One 11 (2016) e0165588, https://doi.org/10.1371/journal.pone.0165588.

[36] T. Patra, S. Bag, R. Kancherla, A. Mondal, A. Dey, S. Pimparkar, S. Agasti, A. Modak, D. Debabrata Maiti, Palladium-catalyzed directed para C-H functionalization of phenols, *Angew. Chem. Int. Ed.* 55 (2016) 7751 –7755, https://doi.org/10.1002/anie.201601999.

[37] Y. Uto, A. Hirata, T. Fujita, S. Takubo, H. Nagasawa, H. Hori, First total synthesis of artepillin C established by o,o'-diprenylation of p-halophenols in water, J. Org. Chem. 67 (2002) 2355-2357, https://doi.org/10.1021/jo0056904.

[38] K. Kantee, V. Rukachaisirikul, K. Tadpetch, Synthesis of tetrahydropyranyl diarylheptanoids from *Dioscorea villosa*, *Tetrahedron Lett.* 57 (2016) 3505–3509, https://doi.org/10.1016/j.tetlet.2016.06.102.

[39] CLSI, Methods for dilution antimicrobial susceptibility tests for bacteria that grow aerobically. 11th ed. Approved Standard M07, Clinical and Laboratory Standards Institute, Wayne, Pensilvania, 2018.

[40] E.A. Duarte, M.B. Santiago, N.B.S. Silva, C.H.G. Martins, C.C. Gatto, Crystal design, spectroscopic analyses and antibacterial study of new carbazate ligands and their Cu(II) complexes, Inorg. Chim. Acta 549 (2023) 121421, https://doi.org/10.1016/j.ica.2023.121421.

[41] S.D. Sarker, L. Nahar, Y. Kumarasamy, Microtitre plate-based antibacterial assay incorporating resazurin as an indicator of cell growth, and its application in the in vitro antibacterial screening of phytochemicals, *Methods* 42 (2007) 321-324, https://doi.org/10.1016/j.ymeth.2007.01.006.

[42] J.M.P. Stewart, Optimization of parameters for semi-empirical methods V: modification of NDDO approximations and application to 70 elements, J. Mol. Model. 13 (2007) 1173-1213, https://doi.org/10.1007/s00894-007-0233-4.

[43] S.C. Feil, S. Lawerence, T.D. Mulhern, J.K. Holien, E.M. Hotze, S. Farrand, R.K. Tweten, M.W. Parker, Structure of the lectin regulatory domain of the cholesterol-dependent cytolysin

lectinolysin reveals the basis for its lewis antigen specificity, Structure 20(2) (2012) 248-258, https://doi.org/10.1016/j.str.2011.11.017.

[44] O. Makhlynets, A.K. Boal, D.V. Rhodes, T. Kitten, A.C. Rosenzweig, J. Stubbe, *Streptococcus sanguinis* class Ib ribonucleotide reductase: high activity with both iron and manganese cofactors and structural insights, J. Biol. Chem. 289(9) (2014) 6259-6272, https://doi.org/10.1074/jbc.M113.533554.

[45] K. Ito, S. Ito, T. Shimamura, S. Weyand, Y. Kawarasaki, T. Miwaka, K. Abe, T. Kobayashi, A.D. Cameron, S. Iwata, Crystal structure of glucansucrase from the dental caries pathogen *Streptococcus mutans*, J. Mol. Biol. 408 (2011) 177-186, https://doi.org/10.1016/j.jmb.2011.02.028.

[46] MOE, Molecular Operating Environment (MOE), 2013.08, Chemical Computing Group Inc., Montreal, QC, Canada, 2014.

[47] I. Daoud, N. Melkemi, T. Salah, S. Ghalem, Combined QSAR, molecular docking and molecular dynamics study on new Acetylcholinesterase and Butyrylcholinesterase inhibitors, Comput. Biol. Chem. 74 (2018) 304-326, https://doi.org/10.1016/j.compbiolchem.2018.03.021.

[48] I. Daoud, F. Mesli, N. Melkemi, S. Ghalem, T. Salah, Discovery of potential SARS-CoV 3CL protease inhibitors from approved antiviral drugs using: virtual screening, molecular docking, pharmacophore mapping evaluation and dynamics simulation, J. Biomol. Struct. Dyn. 40(23) (2021) 12574-12591, https://doi.org/10.1080/07391102.2021.1973563.

[49] M. Bajda, A. Więckowska, M. Hebda, N. Guzior, C.A. Sotriffer, B. Malawska, Structure-based search for new inhibitors of cholinesterases, Int. J. Mol. Sci. 14(3) (2013) 5608-5632, https://doi.org/10.3390/ijms14035608.

554 [50] S.D. Bond, B.J. Leimkuhler, B.B. Laird, The Nosé-Poincaré method for constant temperature
555 molecular dynamics, J. Comp. Phys. 151 (1999) 114-134,
556 https://doi.org/10.1006/jcph.1998.6171.
557 [51] A.A. Parikesit, H. Zahroh, A.S. Nugroho, A. Hapsari, U.S.F. Tambunan, The computation of
558 cyclic peptide with prolin-prolin bond as fusion inhibitor of DENV envelope protein through
559 molecular docking and molecular dynamics simulation, arXiv q-bio (2015) arXiv:1511.01388,
560 https://doi.org/10.48550/arXiv.1511.01388.
561 [52] OriginLab, OriginPro 9.1, OriginLab Corporation, Northampton, MA 01060, United States,
562 2014.
563 [53] A. Daina, O. Michielin, V. Zoete, SwissADME: a free web tool to evaluate pharmacokinetics,
564 drug-likeness and medicinal chemistry friendliness of small molecules, Sci. Rep. 7(1) (2017)
565 1-13, https://doi.org/10.1038/srep42717.
566 [54] D.E. Pires, T.L. Blundell, D.B. Ascher, pkCSM: predicting small-molecule pharmacokinetic
567 and toxicity properties using graph-based signatures, J. Med. Chem. 58(9) (2015) 4066-4072,
568 https://doi.org/10.1021/acs.jmedchem.5b00104.
569 [55] T.A.S. Oliveira, M.B. Santiago, V.H.P. Santos, E.O. Silva, C.H.G. Martins, A.E.M. Crotti,
570 Antibacterial activity of essential oils against oral pathogens, Chem. Biodiv. 19 (2022)
571 e202200097, https://doi.org/10.1002/cbdv.202200097.
572 [56] J.L. Rios, M.C. Recio, Medicinal plants and antimicrobial activity, J. Ethnopharmacol. 100
573 (2005) 80–84, https://doi.org/10.1016/j.jep.2005.04.025.
574 [57] M. Saleem, M. Nazir, M.S. Ali, H. Hussain, Y.S. Lee, N. Riaz, A. Jabbar, Antimicrobial natural
575 products: an update on future antibiotic drug candidates, Nat. Prod. Rep. 27 (2010) 238–254,
576 https://doi.org/10.1039/b916096e.

[58] E.M. Abdallah, B.Y. Alhatlani, R.P. Menezes, C.H.G. Martins, Back to nature: medicinal plants as promising sources for antibacterial drugs in the post-antibiotic era, Plants 12(17) (2023) 3077, https://doi.org/10.3390/plants12173077.

[59] S. Tazawa, T. Warashina, T. Noro, T. Miyase, Studies on the constituents of Brazilian Propolis, Chem. Pharm. Bull. 46(9) (1998) 1477-1479, https://doi.org/10.1248/CPB.46.1477.

[60] A. Schmitt, H. Telikepalli, L.A. Mitscher, Plicatin B, the antimicrobial principle of *Psoralea juncea*, Phytochemistry 30(11) (1991) 3569-3570, https://doi.org/10.1016/0031-9422(91)80067-b.

[61] X.L. Liu, Y.J. Xu, M.L. Go, Functionalized chalcones with basic functionalities have antibacterial activity against drug sensitive *Staphylococcus aureus*, Eur. J. Med. Chem. 43 (2008) 1681-1687, https://doi.org/10.1016/j.ejmech.2007.10.007.

[62] I. Kubo, H. Muroi, A. Kubo, Structural functions of antimicrobial long-chain alcohols and phenols, Bioorg Med Chem. 3 (1995) 873-880, https://doi.org/10.1016/0968-0896(95)00081-q.

[63] F.M.F. Roleira, C. Siquet, E. Orrù, E.M. Garrido, J. Garrido, N. Milhazes, G. Podda, F. Paiva-Martins, S. Reis, R.A. Carvalho, Lipophilic phenolic antioxidants: Correlation between antioxidant profile, partition coefficients and redox properties, Bioorg. Med. Chem. 18 (2010) 5816-5825, https://doi.org/10.1016/j.bmc.2010.06.090.

[64] S. Oufensou, S. Casalini, V. Balmas, P. Carta, W. Chtioui, M.A. Dettori, D. Fabbri, Q. Migheli, G. Delogu, Prenylated *trans*-cinnamic esters and ethers against clinical *Fusarium* spp.: repositioning of natural compounds in antimicrobial discovery, Molecules 26(3) (2021) 658, https://doi.org/10.3390/molecules26030658.

[65] C. Araya-Cloutier, J.-P. Vincken, M.G.M. van de Schans, J. Hageman, G. Schafternaar, H.M.W. den Besten, H. Gruppen, QSAR-based molecular signatures of prenylated (iso)flavonoids

underlying antimicrobial potency against and membrane-disruption in Gram positive and Gram negative bacteria, Sci. Rep. 8 (2018) 9267, https://doi.org/10.1038/s41598-018-27545-4.

[66] A. Imberty, K.D. Hardman, J.P. Carver, S. Perez, Molecular modelling of protein-carbohydrate interactions. Docking of monosaccharides in the binding site of concanavalin A, Glycobiology 1(6) (1991) 631-642, https://doi.org/10.1093/glycob/1.6.631.

[67] R.C. Wade, P.J. Goodford, The role of hydrogen-bonds in drug binding, Progr. Clin. Biol. Res. 289 (1989) 433-444,

[68] L.P. Fernandes, J.M.B. Silva, D.O.S. Martins, M.B. Santiago, C.H.G. Martins, A.C.G. Jardim, G.S. Oliveira, M. Pivatto, R.A.C. Souza, E.F. Franca, V.M. Deflon, A.E.H. Machado, C.G. Oliveira, Fragmentation study, dual anti-bactericidal and anti-viral effects and molecular docking of cobalt (III) complexes, Int. J. Mol. Sci. 21 (2020) 8355, https://doi.org/10.3390/ijms21218355.

[69] J.J. Velarde, A. Piai, I.J. Lichtenstein, N.N. Lynskey, J.J. Chou, M.R. Wessels, Structure of the *Streptococcus pyogenes* NAD^+ Glycohydrolase translocation domain and its essential role in toxin binding to oropharyngeal keratinocytes, J. Bacteriol. 204(1) (2022) e00366-21, https://doi.org/10.1128/JB.00366-21.

[70] B. Nijampatnam, H. Zhang, X. Cai, S.M. Michalek, H. Wu, S.E. Velu, Inhibition of *Streptococcus mutans* biofilms by the natural stilbene piceatannol through the inhibition of glucosyltransferases, ACS Omega 3(7) (2018) 8378-8385, https://doi.org/10.1021/acsomega.8b00367.

[71] L. Atta, R. Khalil, K.M. Khan, M. Zehra, F. Saleem, M. Nur-e-Alam, Z. Ul-Haq, Virtual screening, synthesis and biological evaluation of *Streptococcus mutans* mediated biofilm inhibitors, Molecules 27(4) (2022) 1455, https://doi.org/0.3390/molecules27041455.

[72] Y. Liao, M. Zhang, X. Lin, F. Yan, Diaryl urea derivative molecule inhibits cariogenic *Streptococcus mutans* by affecting exopolysaccharide synthesis, stress response, and nitrogen

metabolism, Front. Cell. Infect. Microbiol. 12 (2022) 904488, https://doi.org/10.3389/fcimb.2022.904488.

[73] N. Roy, B. Ghosh, D. Roy, B. Bhaumik, M.N. Roy, Exploring the inclusion complex of a drug (umbelliferone) with α-cyclodextrin optimized by molecular docking and increasing bioavailability with minimizing the doses in human body, ACS Omega 5 (2020) 30243-30251, https://doi.org/10.1021/acsomega.0c04716.

[74] R. Djebaili, S. Kenouche, I. Daoud, N. Melkemi, A. Belkadi, F. Mesli, Investigation of [^{3}H]diazepam derivatives as allosteric modulators of GABAA receptor $\alpha_1\beta_2\gamma_2$ subtypes: combination of molecular docking/dynamic simulations, pharmacokinetics/drug-likeness prediction, and QSAR analysis, Struct. Chem. 34(3) (2022) 791-823, https://doi.org/10.1007/s11224-022-02029-4.

638 **Table 1:** Some information related to studied targets.

639

Targets PDB	Methods	Organism	Chain	Sequence length	Resolution (Å)	Native-ligands
3LE0	X-ray diffraction	*Streptococcus mitis*	A	153	1.91	GOL
4N82	X-ray diffraction	*Streptococcus sanguinis*	A, B, C, D, E, F	178	1.88	FMN
3AIC	X-ray diffraction	*Streptococcus mutans*	A, B, C, D, E,	488	3.11	PRD

640

641 **Table 2.** Minimum Inhibitory Concentration (MIC) and *Minimum Bactericidal Concentrations* (MBC) values (µg/mL / mM) of compounds **2-9**, and **11-13**,*

Compound	*Enterococcus faecalis* ATCC 4082	*Lactobacillus paracasei* ATCC 11578	*Streptococcus salivarius* ATCC 25975	*Streptococcus sobrinus* ATCC 33478	*Streptococcus mitis* ATCC 49456	*Streptococcus sanguinis* ATCC 10556	*Streptococcus mutans* ATCC 25175
2 (plicatin B)	500 (2.03)	500 (2.03)	62.5 (0.25)	62.5 (0.25)	31.2 (0.13)	31.2 (0.13)	31.2 (0.13)
	500 (2.03)	*1000 (4.06)*	*250 (1.01)*	*62.5 (0.25)*	*31.2 (0.13)*	*31.2 (0.13)*	*31.2 (0.51)*
3	>2000 (>5.23)	>2000 (>5.23)	2000 (5.23)	2000 (5.23)	500 (1.31)	1000 (2.61)	>2000 (5.23)
	>2000(>5.23)	*>2000(>5.23)*	*>2000(>5.23)*	*>2000(>5.23*	*1000 (2.61)*	*2000 (5.23)*	*>2000 (5.23)*
4	>2000 (8.12)	>2000 (8.12)	>2000 (8.12)	>2000 (8.12)	1000 (4.06)	>2000 (8.12)	>2000 (8.12)
	>2000(>8.12)	*>2000(>8.12)*	*>2000(>8.12)*	*>2000(>8.12)*	*2000 (8.12)*	*>2000(>8.12)*	*>2000(>8.12)*
5 (artepillin C)	>2000 (>6.66)	500 (1.66)	1000 (3.33)	500 (1.66)	125 (0.41)	500 (1.66)	500 (1.66)
	>2000(>6.66)	*1000 (3.33)*	*2000 (6.66)*	*2000 (6.66)*	*1000 (3.33)*	*1000 (3.33)*	*2000 (6.66)*
6 (drupanin)	1000 (3.09)	500 (1.55)	250 (0.77)	125 (0.39)	250 (0.77)	250 (0.77)	125 (0.39)
	1000 (3.09)	*500 (1.55)*	*500 (1.55)*	*125 (0.39)*	*250 (0.77)*	*250 (0.77)*	*250 (0.77)*
7	500 (2.15)	1000 (4.31)	1000 (4.31)	1000 (4.31)	500 (2.15)	500 (2.15)	1000 (4.31)
	>2000(>8.61)	*2000 (8.61)*	*2000 (8.61)*	*1000 (4.31)*	*500 (2.15)*	*500 (2.15)*	*2000 (8.61)*
8	125 (0.50)	62.5 (0.25)	62.5 (0.25)	125 (0.50)	31.25 (0.12)	62.5 (0.25)	62.5 (0.25)
	125 (0.50)	*250 (1.0)*	*62.5 (0.25)*	*125 (0.50)*	*31.25 (0.12)*	*62.5 (0.25)*	*62.5 (0.25)*
9	>2000 (8.0)	>2000 (8.0)	1000 (4.0)	1000 (4.0)	500 (2.0)	1000 (4.0)	2000 (8.0)
	>2000 (8.0)	*>2000 (8.0)*	*2000 (8.0)*	*1000 (4.0)*	*1000 (4.0)*	*1000 (4.0)*	*2000 (8.0)*
11	2000 (9.16)	2000 (9.16)	62.5 (0.29)	2000 (9.16)	500 (2.29)	1000 (4.58)	1000 (4.58)
	>2000 (>9.1)	*>2000 (>9.1)*	*125 (0.57)*	*2000 (9.16)*	*1000 (4.58)*	*2000 (9.16)*	*2000 (9.16)*
12	1000 (3.26)	500 (1.63)	500 (1.63)	250 (0.82)	62.5 (0.20)	500 (1.63)	500 (1.63)
	2000 (6.53)	*1000 (3.26)*	*500 (1.63)*	*500 (1.63)*	*125 (0.41)*	*1000 (3.26)*	*500 (1.63)*
13	>2000 (8.46)	>2000 (8.46)	>2000 (8.46)	>2000 (8.46)	250 (1.06)	1000 (4.23)	>2000 (8.46)
	>2000 (8.46)	*>2000 (8.46)*	*>2000 (8.46)*	*>2000 (8.46)*	*1000 (4.23)*	*1000 (4.23)*	*>2000 (8.46)*
Chlorhexidine	3.69 (7.30)	1.84 (3.64)	0.92 (1.82)	1.84 (3.64)	3.69 (7.30)	3.69 (7.30)	0.92 (1.82)
	3.69 (7.30)	*1.84 (3.64)*	*0.92 (1.82)*	*1.84 (3.64)*	*3.69 (7.30)*	*3.69 (7.30)*	*0.92 (1.82)*

642 * Compounds **1, 10,** and **14** were inactive (MIC > 1000 µg/mL against all the tested bacteria and were not included).

Table 2.Table 3. Docking results of compounds **2** and **8** docked into *S. mitis* (PDB ID: 3LE0), *S. sanguinis* (PDB ID: 4N82), and ***S. mutans*** **(PDB ID: 3AIC)** targets.

Compds	S-Score (kcal/mol)	RMSD (Å)	Bonds between atoms of compounds and active site residues					
			Atom of compound	Involved receptor Atoms	Involved receptor Residues	Category	Type of interaction	Distance (Å)
S. mitis **(PDB ID: 3LE0)**								
4	-4.228	2.997	O	HH11	ARG120(A)	Hydrogen Bond	Conventional H-Bond	2.28
			H	NE2	HIS85(A)	Hydrogen Bond	Conventional H-Bond	1.98
			/	NH2	ARG112(A)	Electrostatic	Pi-Cation	4.01
			C	/	TYR62(A)	Hydrophobic	Pi-Pi T-shaped	5.02
			C	/	VAL117(A)	Hydrophobic	Alkyl	4.91
5	-4.476	2.932	H	NE2	HIS85(A)	Hydrogen Bond	Conventional H-Bond	2.23
			H	OD1	ASP114(A)	Hydrogen Bond	Carbon H-Bond	2.87
			H	OD2	ASP77(A)	Hydrogen Bond	Carbon H-Bond	2.90
			H	OD1	ASP114(A)	Hydrogen Bond	Carbon H-Bond	2.95
			/	NH2	ARG112(A)	Electrostatic	Pi-Cation	3.88
			C	/	VAL117(A)	Hydrophobic	Alkyl	5.38
Native ligand (GOL)	-3.655	2.149	O1	HH11	ARG120(A)	Hydrogen Bond	Conventional H-Bond	2.30
			O3	HH11	ARG112(A)	Hydrogen Bond	Conventional H-Bond	2.21
			H12	NE2	HIS85(A)	Hydrogen Bond	Carbon H-Bond	2.73
S. sanguinis **(PDB ID: 4N82)**								
4	-6.156	2.071	O	H	ASN104(A)	Hydrogen Bond	Conventional H-Bond	2.37
			O	HA3	GLY103(A)	Hydrogen Bond	Carbon H-Bond	2.93
			/	O	THR63(A)	Other	Pi-Lone Pair	2.94
			/	/	PHE107(A)	Hydrophobic	Pi-Pi Stacked	3.51
			C	/	MET132(A)	Hydrophobic	Alkyl	5.00
			C	/	PRO62(A)	Hydrophobic	Alkyl	4.90
			C	/	TYR64(A)	Hydrophobic	Alkyl	4.67
5	-5. 575	1.283	O	H	ASN104(A)	Hydrogen Bond	Conventional H-Bond	2.77
			H	O	LEU65(A)	Hydrogen Bond	Carbon H-Bond	2.85
			/	O	TYR63(A)	Other	Pi-Lone Pair	2.95
			/	/	PHE107(A)	Hydrophobic	Pi-Pi Stacked	3.54
			C	/	PRO62(A)	Hydrophobic	Alkyl	5.02
Native ligand (FMN)	-6.671	1.034	O1P	H	LEU11(A)	Hydrogen Bond	Conventional H-Bond	2.15
			O3P	H	SER12(A)	Hydrogen Bond	Conventional H-Bond	2.29
			O3P	HG	SER12(A)	Hydrogen Bond	Conventional H-Bond	1.62
			O3P	H	GLY13(A)	Hydrogen Bond	Conventional H-Bond	2.02
			O3P	H	ASN14(A)	Hydrogen Bond	Conventional H-Bond	1.78
			O2P	H	THR15(A)	Hydrogen Bond	Conventional H-Bond	2.27
			O2P	HG1	THR15(A)	Hydrogen Bond	Conventional H-Bond	1.73
			O1P	HH	TYR64(A)	Hydrogen Bond	Conventional H-Bond	1.78
			HO3	OH	TYR64(A)	Hydrogen Bond	Conventional H-Bond	2.90
			HO4	O	SER102(A)	Hydrogen Bond	Conventional H-Bond	2.86
			/	/	PHE107(A)	Hydrophobic	Pi-Pi Stacked	5.92
			/	/	PHE107(A)	Hydrophobic	Pi-Pi Stacked	4.39
			/	/	PHE107(A)	Hydrophobic	Pi-Pi Stacked	3.45
			C7M	/	LEU65(A)	Hydrophobic	Alkyl	4.05
			C7M	/	PHE107(A)	Hydrophobic	Pi-Alkyl	3.93
			C8M	/	PHE107(A)	Hydrophobic	Pi-Alkyl	4.29
S. mutans **(PDB ID: 3AIC)**								
4	-5.049	2.296	O	HE2	HIS587(A)	Hydrogen Bond	Conventional H-Bond	2.04
			H	OD1	ASP909(A)	Hydrogen Bond	Carbon H-Bond	2.85
			H	OD1	ASP909(A)	Hydrogen Bond	Carbon H-Bond	2.74

			/	OE2	GLU515(A)	Electrostatic	Pi-Anion	3.75
			C	/	LEU382(A)	Hydrophobic	Alkyl	4.96
			C	/	HIS587(A)	Hydrophobic	Pi-Alkyl	5.06
			C	/	TYR610(A)	Hydrophobic	Pi-Alkyl	5.40
			C	/	TYR916(A)	Hydrophobic	Pi-Alkyl	4.63
			/	/	LEU433(A)	Hydrophobic	Pi-Alkyl	5.32
5	-5.042	2.622	H	OD1	ASN481(A)	Hydrogen Bond	Carbon H-Bond	2.65
			H	O	GLU515(A)	Hydrogen Bond	Carbon H-Bond	2.66
			/	OD2	ASP588(A)	Electrostatic	Pi-Anion	4.78
			C	/	TRP517(A)	Hydrophobic	Pi-Alkyl	4.75
			C	/	HIS587(A)	Hydrophobic	Pi-Alkyl	5.29
			C	/	HIS587(A)	Hydrophobic	Pi-Alkyl	5.37
			C	/	TYR916(A)	Hydrophobic	Pi-Alkyl	4.88
			C	/	TYR916(A)	Hydrophobic	Pi-Alkyl	4.07
Native ligand (PRD)	-6.674	2.513	O2B	HH21	ARG475(A)	Hydrogen Bond	Conventional H-Bond	2.43
			O2B	HE2	HIS587(A)	Hydrogen Bond	Conventional H-Bond	2.49
			O3B	HE2	HIS587(A)	Hydrogen Bond	Conventional H-Bond	2.26
			H8	OD2	ASP424(A)	Hydrogen Bond	Conventional H-Bond	2.08
			H2	OD1	ASN481(A)	Hydrogen Bond	Conventional H-Bond	2.37
			H6	OE1	GLU515(A)	Hydrogen Bond	Conventional H-Bond	2.14
			H16	OD2	ASP588(A)	Hydrogen Bond	Conventional H-Bond	1.75
			H25	OD2	ASP477(A)	Hydrogen Bond	Conventional H-Bond	2.26
			H4	OD2	ASP909(A)	Hydrogen Bond	Carbon H-Bond	2.53
			H5	OE2	GLU515(A)	Hydrogen Bond	Carbon H-Bond	2.69
			H14	OE1	GLU515(A)	Hydrogen Bond	Carbon H-Bond	2.36
			H15	OD1	ASP477(A)	Hydrogen Bond	Carbon H-Bond	2.74
			H17	OD2	ASP588(A)	Hydrogen Bond	Carbon H-Bond	2.59
			H24	OD2	ASP909(A)	Hydrogen Bond	Carbon H-Bond	2.74
			H9	OD2	ASP588(A)	Electrostatic	Attractive Charge	2.57
			H8	OE2	GLU515(A)	Electrostatic	Attractive Charge	2.33
			H8	OD2	ASP588(A)	Electrostatic	Attractive Charge	2.50
			N4A	OD1	ASP477(A)	Electrostatic	Attractive Charge	5.31

644

645

646

647

Table 4 Physicochemical properties and Drug-likeness predictions of compounds 4 and 5.

Compounds	Physicochemical Property						Medicinal Chemistry		
							Rules druglikeness		
	TPSA (Å^2)	n-ROT	MW (g/mol)	MLog P / WLogP	n-HA	n-HD	Lipinski	Veber	Egan
	(0~140)	(0~11)	(100~500)	(0~5)	(0~12)	(0~7)			
4	39.42	2	225.25	1.49 / 2.40	3	0	Accepted	Accepted	Accepted
5	30.19	1	223.27	2.33 / 3.01	2	0	Accepted	Accepted	Accepted

TPSA: Topological Polar Surface Area**, n-ROT:** Number Of Rotatable, **MW:** Molecular Weight, **Log P:** Logarithm of partition coefficient of compound between n-octanol and water, **n-HA:** Number of hydrogen bond acceptors**, n-HD:** Number of hydrogen bonds donors.

Table 5 ADMET/pharmacokinetic properties of compounds L4 and L5.

ADME	*Parameters*	*Compounds*	
		4	**5**
Absorption	**Caco2 (10^{-6}cm/s)**	1.178	1.417
	HIA (%)	99.207	97.682
Distribution	**CNS (log PS)**	-1.800	-1.692
	BBB (log BB)	0.311	0.030
Metabolism	**CYP1A2 inhibitor**	Yes	Yes
	CYP2C19 Inhibitor	No	No
	CYP2D6 inhibitor	No	No
	CYP2D6 substrate	No	No
	CYP3A4 substrate	No	No
Excretion	**Renal OCT2 substrate**	No	No
	Total Clearance (log mL/min/kg)	0.744	0.780
Toxicity	**hERG I and II inhibitors**	No	No
	Hepatotoxicity	No	No

Caco-2: Colon adenocarcinoma, **HIA:** Human intestinal absorption, **CNS:** Central Nervous System permeability, **BBB:** Blood–Brain Barrier permeability, **Renal OCT2 substrate:** Organic cation transporter 2, **hERG:** Human Ether-à-go-go-Related Gene.

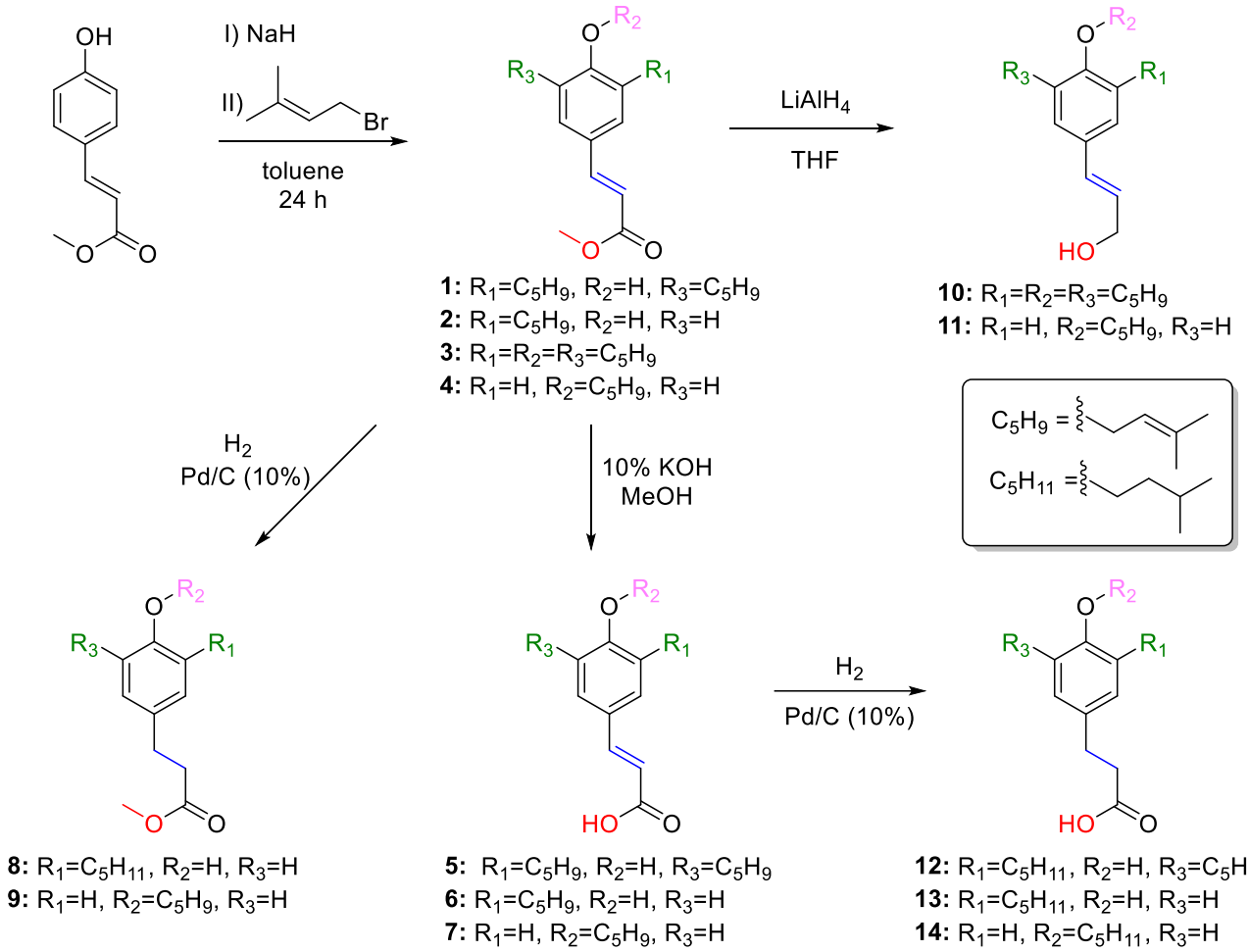

1: $R_1=C_5H_9$, $R_2=H$, $R_3=C_5H_9$
2: $R_1=C_5H_9$, $R_2=H$, $R_3=H$
3: $R_1=R_2=R_3=C_5H_9$
4: $R_1=H$, $R_2=C_5H_9$, $R_3=H$

10: $R_1=R_2=R_3=C_5H_9$
11: $R_1=H$, $R_2=C_5H_9$, $R_3=H$

8: $R_1=C_5H_{11}$, $R_2=H$, $R_3=H$
9: $R_1=H$, $R_2=C_5H_9$, $R_3=H$

5: $R_1=C_5H_9$, $R_2=H$, $R_3=C_5H_9$
6: $R_1=C_5H_9$, $R_2=H$, $R_3=H$
7: $R_1=H$, $R_2=C_5H_9$, $R_3=H$

12: $R_1=C_5H_{11}$, $R_2=H$, $R_3=C_5H_{11}$
13: $R_1=C_5H_{11}$, $R_2=H$, $R_3=H$
14: $R_1=H$, $R_2=C_5H_{11}$, $R_3=H$

Scheme 1. Synthesis of compounds **1-14.**

657 **Figure 1.** Chemical structures of drupanin (**I**) and artepillin C (**II**).

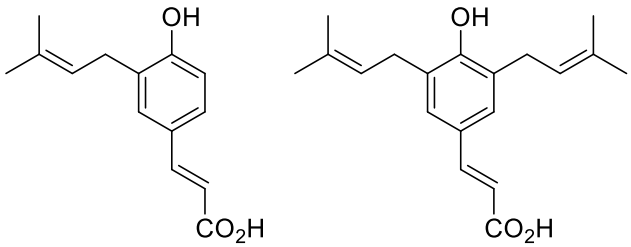

658 **I** **II**

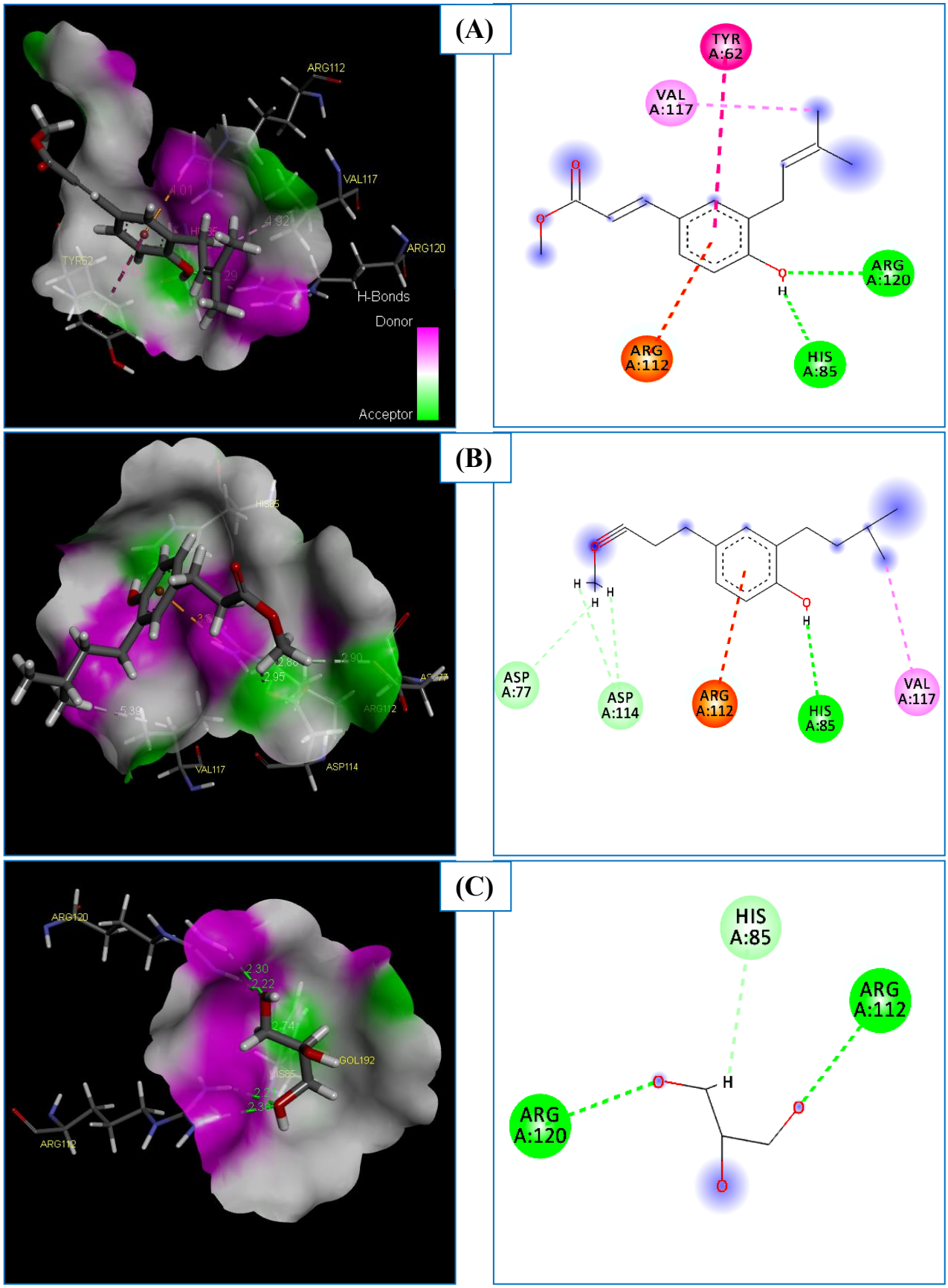

Figure 2. 3D and 2D diagrams of Interaction between, (**A**): the compound **2** and *S. mitis*; (**B**): the compound **8** with *S. mitis*; (**C**): the native ligand (GOL) and *S. mitis*;

659

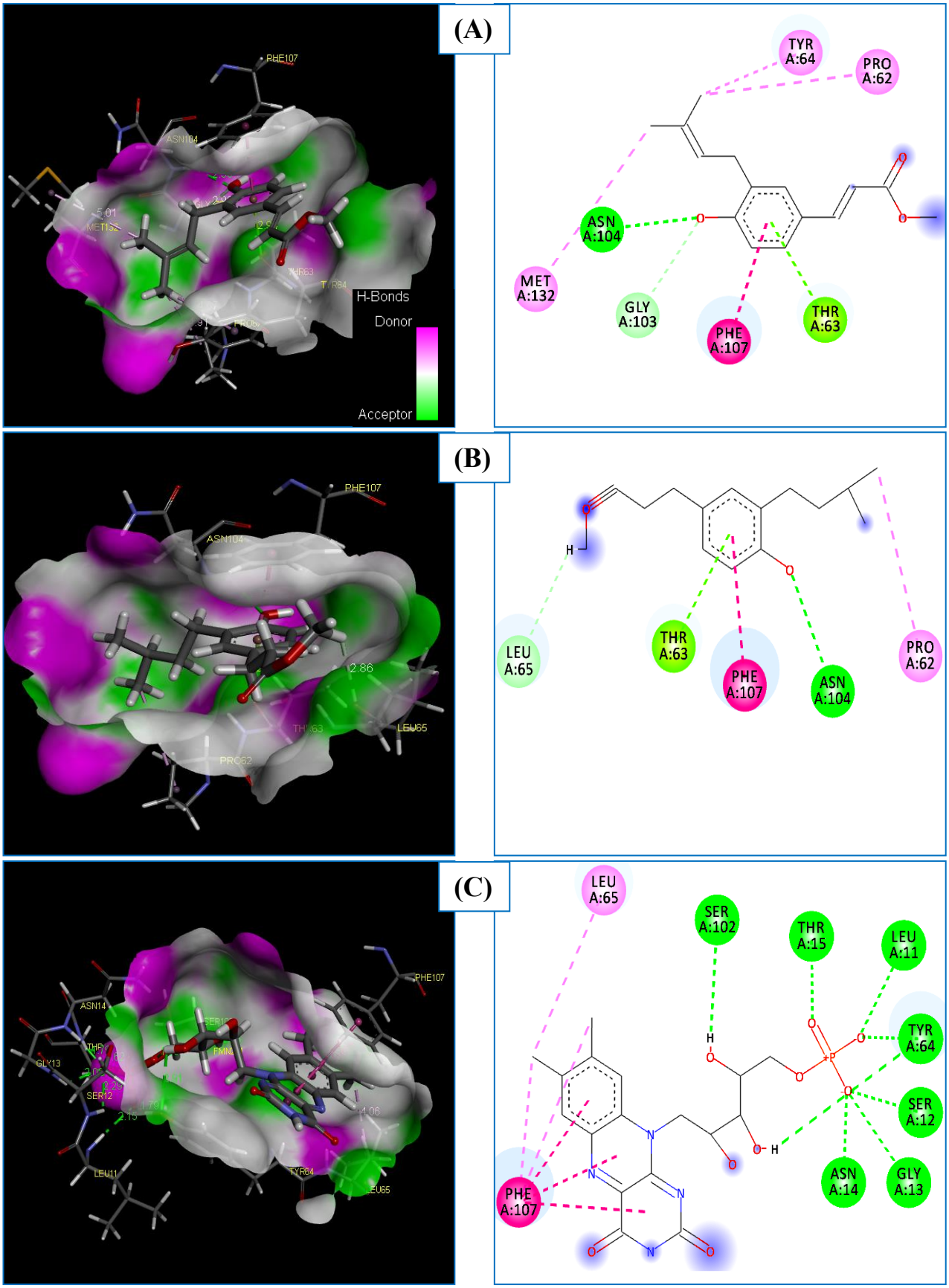

Figure 3. 3D and 2D diagrams of Interaction between, (**D**): the compound **2** and *S. sanguinis*; (**E**): the compound **8** and *S. sanguinis*; (**F**): the native ligand (FMN) and *S. sanguinis*.

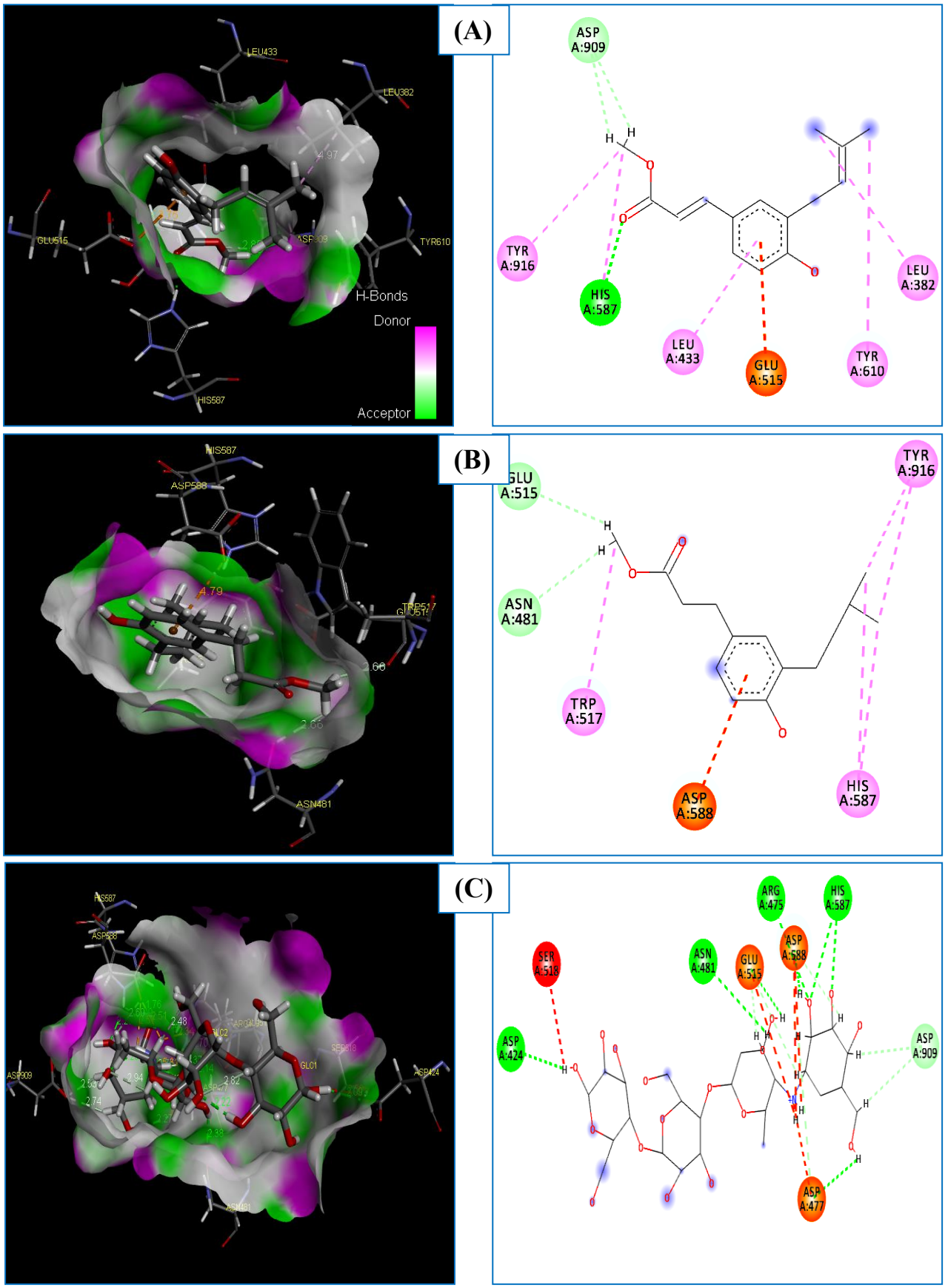

Figure 4. 3D and 2D diagrams of Interaction between, (**G**): the compound **2** and *S. mutans*; (**H**): the compounds **8** with *S. mutans*; (**I**): the native ligand **(**PRD**)** and *S. mutans*.

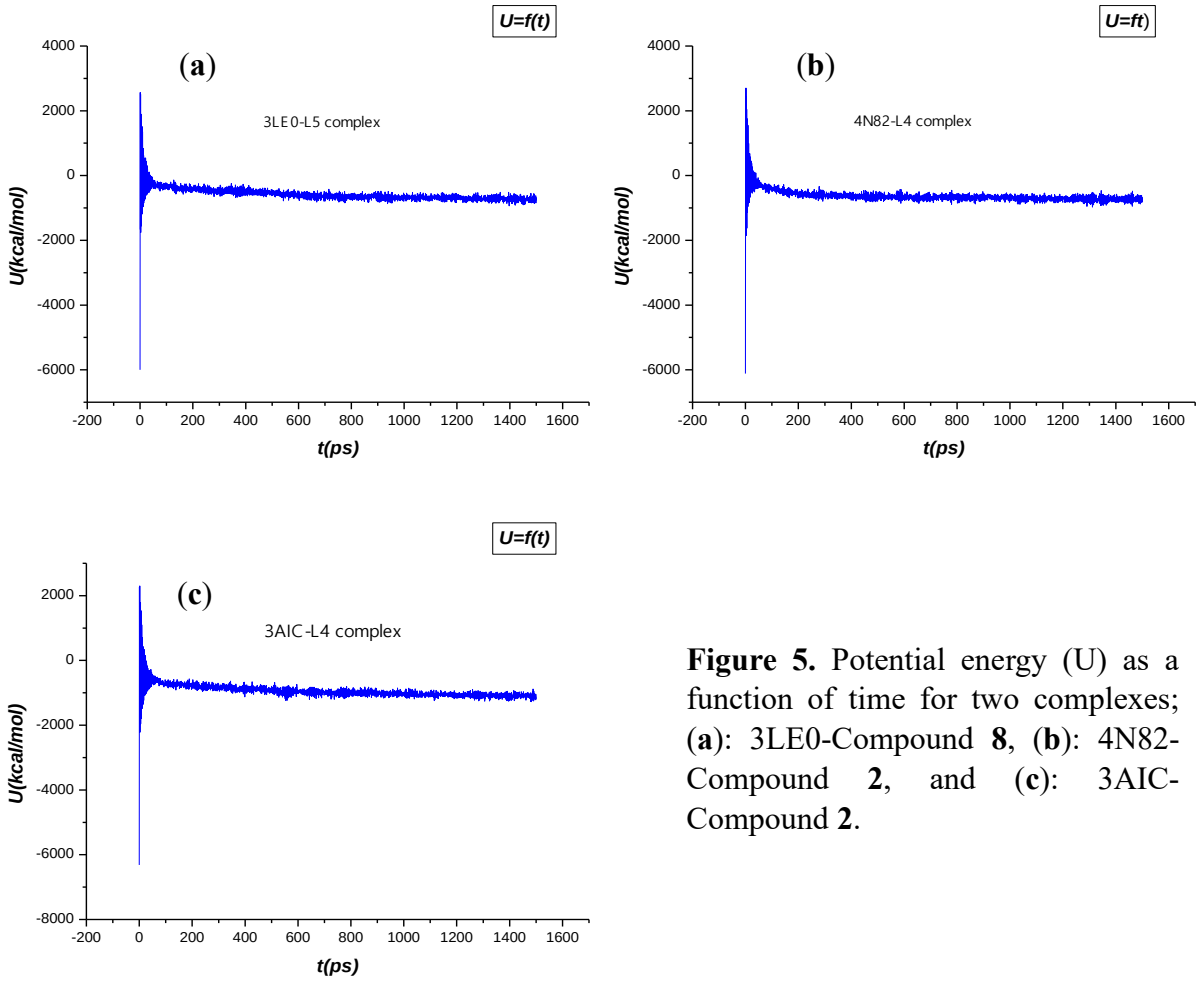

Figure 5. Potential energy (U) as a function of time for two complexes; (**a**): 3LE0-Compound **8**, (**b**): 4N82-Compound **2**, and (**c**): 3AIC-Compound **2**.